Journal of Nuclear Materials 394 (2009) 20–25

Contents lists available at ScienceDirect

Journal of Nuclear Materials

journal homepage: www.elsevier.com/locate/jnucmat

# Effect of chemical potential of carbon on phase transformation and corrosion of JLF-1 steel in a static lithium

Qi Xu [a], Masatoshi Kondo [a,b,*], Takuya Nagasaka [a,b], Takeo Muroga [a,b], Olga Yeliseyeva [c]

[a] The Graduate University for Advanced Studies, Toki, Gifu 509-5292, Japan
[b] National Institute for Fusion Science, Toki, Gifu 509-5292, Japan
[c] Physical–Mechanical Institute of National Academy of Sciences of Ukraine, 5, Naukova Str., L'viv 79053, Ukraine

ARTICLE INFO

*Article history:*
Received 29 September 2008
Accepted 1 August 2009

ABSTRACT

The corrosion and the phase transformation of RAFM (Reduced Activation Ferritic/Martensitic) steel, JLF-1(Fe–9Cr–2W–0.1C), in static lithium (Li) were investigated. The specimens were exposed to static Li at 600 °C for 250 h. The carbon potential in Li was controlled by the carbide formation on inner surface of the crucible, which was made of Mo and Nb. These materials were expected to form stable carbide, and worked as carbon trap in Li, which resulted in the decrease in the carbon potential of Li. The effect of low carbon potential on the corrosion and the phase transformation was characterized by comparison with the test performed in the crucible made of Fe–9Cr and SUS316L (18Cr–12Ni), which has no effect as carbon traps. The low carbon potential caused by Nb and Mo caused the dissolution of carbon from the surface of JLF-1 specimen to Li. The depth of the phase transformation observed after the test in Nb crucible was deeper than that tested in Mo crucible. This was because the stability of the Nb carbide was larger than that of Mo carbide causing larger driving force for the dissolution of carbides from the surface.


## 1. Introduction

Blanket concepts with liquid lithium (Li) breeder/coolant provide attractive options for high tritium breeding ratio, high efficiency and simplicity of the system [1]. Fe–Cr–W based RAFM (Reduced Activation Ferritic/Martensitic) steels are widely regarded as promising structural materials of the blanket system, because of its low activation properties, radiation resistance and industrial maturity. JLF-1 (Japanese low activation ferritic steel 1, Fe–9Cr–2W) has excellent resistance against neutron exposures in both microstructural and mechanical properties [2], and is a potential candidate for the structural material of blanket.

For the blanket concepts, the compatibility of RAFM with liquid Li is one of the issues. The interaction of alloy elements and Li containing nitrogen impurity has been studied. The corrosion of Fe–Cr–Mn steels and Fe–Cr–Ni steels in liquid Li was investigated in Refs. [3,4], which reported that the corrosion was mainly caused by dissolution of Cr, Ni and Mn from the steels. The interaction mechanism of Cr with nitrogen dissolved in Li was studied in Refs. [5,6].

The corrosion of Ferritic/Martensitic steel in Li is expected to be influenced by the microstructure with carbide precipitates and the lath structure near the surface [7]. However, the data for the corrosion of RAFM in Li is limited.

A series of corrosion tests for JLF-1 in Li was performed, and it was found that the corrosion was caused by the selective dissolution of Cr, W, and C into Li at static condition [8]. The corrosion loss in thermal convection loop test was larger than that at static conditions [9,10]. In these studies, the corroded surface showed the ferritic phase, and indicating the phase transformation from martensitic phase to ferritic one was caused by the Li exposure. It was found that the dissolution of carbon from the steel to the Li caused the phase transformation. However, the effect of chemical potential of carbon in Li on the dissolution of carbon was not made clear.

Decarburization of steel in liquid sodium at low carbon concentration was investigated in Ref. [11]. However, data of the phase transformation in Li was limited. The phase transformation resulted in degradation of mechanical properties. Therefore, the mechanism must be made clear.

The purpose of the present study is to investigate the effect of carbon potential in Li on the phase transformation and corrosion of JLF-1. Carbon potential in Li was controlled by chemical trap to form the stable carbide on the crucible made of Nb and Mo.

* Corresponding author. Address: National Institute for Fusion Science, Fusion Engineering Research Center, 322-6, Toki, Gifu 509-5292, Japan. Tel.: +81 572 58 2139.
*E-mail addresses:* xu.qi@nifs.ac.jp (Q. Xu), kondo.masatoshi@nifs.ac.jp (M. Kondo), nagasaka@nifs.ac.jp (T. Nagasaka), muroga@nifs.ac.jp (T. Muroga), OlgaYeliseyeva@ipm.lviv.ua (O. Yeliseyeva).

0022-3115/$ - see front matter © 2009 Elsevier B.V. All rights reserved.
doi:10.1016/j.jnucmat.2009.08.005

## 2. Experimental conditions

### 2.1. Test material

The test material, JLF-1, is Fe–Cr–W based RAFM steel, with chemical composition (wt.%): 8.93Cr, 1.96W, 0.64Mn, 0.49Ni, 0.21V, 0.10C, 0.015N, and Fe as balance. Ingot of JLF-1 were heat-treated at 1050 °C/3.6ks/air cooled (normalizing) and 780 °C/3.6ks/air cooled (tempering). JLF-1 has martensite lath structure as presented in the previous studies [7,8,10].

The ingot was cut into the specimens by low speed cutter with the size of 26 × 5 × 0.25 mm. Then, the surfaces of the specimens were mechanically polished to remove initial oxide layer before the exposure. The surfaces were finally polished using $Al_2O_3$ powder of 0.05 μm in diameter. This procedure was the same as that in the previous studies [8,10].

### 2.2. Experimental apparatus

The corrosion test apparatus is shown in Fig. 1. The apparatus was the same with that used in the previous studies [8,10]. The impurity in the Li was 0.85Fe–0.12Cr–0.80Ni–0.11Mo–0.31W–65N in the unit of wppm. Ten pieces of specimens were fixed to the specimen holder by the wires, and the holder was placed in the Li. The ratio of Li volume (92 $cm^3$) to total surface area of specimens (27.55 $cm^2$) was around 3.34 (cm). The test apparatus was assembled with specimens and Li in a glove box filled with argon with purity of 99.999%.

### 2.3. Corrosion test conditions

The corrosion tests were performed at the conditions presented in Table 1. The test temperature was slightly higher than that in the outlet of the blanket. The exposure time was determined as 250 h because the corrosion loss became constant after 250 h in the previous study [10]. The materials of crucible, the specimen holder and the wire are presented in Table 1. Four types of these sets were prepared with material of Fe–9Cr, SUS316L (18Cr–12Ni–2Mo), Mo and Nb. These were used as the parameter in the corrosion test to control the carbon potential in Li.

**Table 1**
Corrosion test conditions.

| | Temperature (°C) | Exposure time (h) | Specimen number | Material of crucible | Material of specimen holder and wire |
|---|---|---|---|---|---|
| Test A | 600 | 250 | 10 | Fe–9Cr | Fe wire |
| Test B | 600 | 250 | 10 | SUS316L | SUS316L |
| Test C | 600 | 250 | 10 | Mo | Mo |
| Test D | 600 | 250 | 10 | Nb | Nb |

### 2.4. Control of carbon potential in Li by chemical trap

The chemical potential of carbon in Li was controlled by the formation of carbide on the crucible surfaces. The carbon is assumed to be dissolved as $Li_2C_2$ at low concentration of nitrogen [12]. The possible chemical reactions on the surface for the crucible formation of carbide in each crucible are:

$$6Fe + Li_2C_2 \rightarrow 2Fe_3C + 2Li \quad (Fe—9Cr \text{ and SUS316L crucible}) \quad (1)$$

$$7.667Cr + Li_2C_2 \rightarrow 0.3333Cr_{23}C_6 + 2Li \quad (Fe—9Cr \text{ and SUS316L crucible}) \quad (2)$$

$$4Mo + Li_2C_2 \rightarrow 4MoC_{0.50} + 2Li \quad (Mo \text{ crucible}) \quad (3)$$

$$2Nb + Li_2C_2 \rightarrow 2NbC + 2Li \quad (Nb \text{ crucible}) \quad (4)$$

The reverse reactions of Eqs. (1) and (2) can occurred, and this is the reaction for the dissolution of carbon from the specimens. The Gibbs reaction energy for Eqs. (3) and (4) can be given according to the equations;

$$\Delta_r G_{eq.(3)} = \Delta_r G^0_{eq.(3)} + RT \ln \frac{c_{MoC_{0.5}}{}^4 c_{Li}^2}{c_{Mo}{}^4 c_{Li_2C_2}} \quad (5)$$

$$\Delta_r G_{eq.(4)} = \Delta_r G^0_{eq.(4)} + RT \ln \frac{c_{NbC}{}^2 c_{Li}^2}{c_{Nb}{}^2 c_{Li_2C_2}}, \quad (6)$$

where $\Delta_r G_{eq.(3)}$ and $\Delta_r G_{eq.(4)}$ are the Gibbs reaction energy for Eqs. (3) and (4), respectively. $\Delta_r G^0_{eq.(3)}$ and $\Delta_r G^0_{eq.(4)}$ are the Gibbs reaction energy for standard for the reaction of Eqs. (3) and (4), respectively. These were −60.37 kJ/mol and −221.5 kJ/mol at 900 K, respectively,

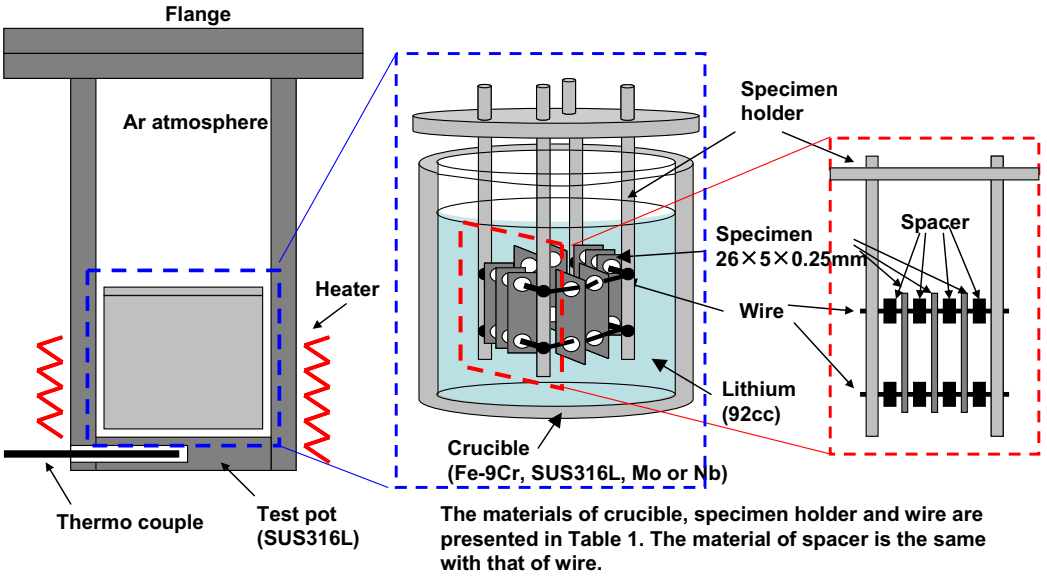


**Fig. 1.** Experimental apparatus for corrosion test in static Li.

[13]. The concentration of NbC, Li and Nb are thought to be unity. $R$ is the gas constant (8.314 J/mol K) and $T$ is the test temperature of 873 K.

Fig. 2 shows the Gibbs reaction energy for the formation of carbide on the inner surface of crucible. It illustrates that Mo and Nb tend to capture the C from Li when Mo and Nb are used as container materials for Li corrosion test. On the other hand, Fe–9Cr and SUS316 crucible does not react with $Li_2C_2$ easily, because the reaction between Fe and $Li_2C_2$ is not spontaneous. Although both Mo and Nb act as C-trap in Li, Nb is a much stronger trap than Mo.

When the reaction reaches to the equilibrium, $\Delta_r G_{eq.(3)}$ and $\Delta_r G_{eq.(4)}$ in Eqs. (5) and (6) are to be zero in equilibrium. Then, $C_{Li2C2}$ in Mo crucible and Nb crucible is estimated as 244.1 mol ppm and $5.506 \times 10^{-5}$ mol ppb, respectively.

The purpose to use the crucible of Fe–9Cr steel is to have standard data for the phase change and corrosion in Li without any effect of carbide formation on the crucible. The SUS316L crucible was used to compare the data of the phase change and corrosion with the previous results [8]. The crucible made of Mo and Nb was used to investigate the effect of low carbon potential on the phase change, where the low potential was made by the equilibrium for the formation of carbide on the crucible inner surface.

### 2.5. Analysis of corrosion and phase transformation after tests

After the exposure, the specimens and the holder were cleaned by water followed by ultrasonic clean in acetone. The weight loss was measured by electro-balance with the accuracy of 0.1 mg.

The surface morphology and composition was analyzed by Scanning Electron Microscope (SEM) equipped with Energy Dispersive X-ray Spectrometer (EDS). The cross section of the specimen was made by the mechanical polish as mentioned in Section 2.1 after the specimen embedded in resin. Then, the lath structure was observed by SEM/EDS after electro etching at 30 V in the pool of 13% $HClO_4$–13% ethyleneglycol monobutyl ether–10% ethanol–64% acetic acid. The etching procedure was done for all the cross sectional analysis to investigate the phase transformation.

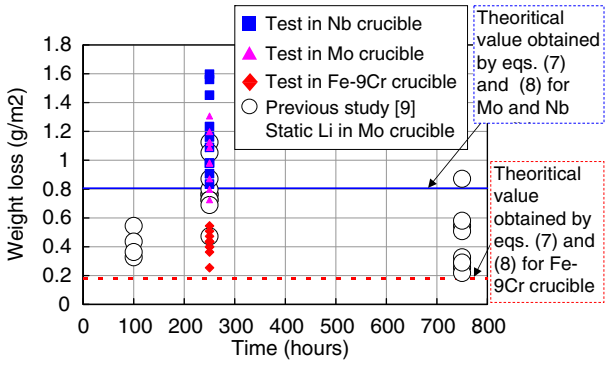


**Fig. 3.** Weight loss of specimens in the present and previous studies (theoretical values are explained in Section 3.3).

Vickers hardness test with load of 10 g was carried out to investigate the change of mechanical properties. The hardness test was done in the cross section of the specimens. The data of the certain depth was obtained for three times and averaged. The error was less than 3%.

The change of nitrogen concentration before and after the test was checked by means of ammonia extraction method [14].

## 3. Results and discussions

The results of SEM analysis for the surface and the cross section are shown in Figs. 4 and 5, respectively.

For the comparison, the surface condition of specimen before the exposure is shown in Fig. 4E. The hardness change of specimen surface as a function of depth is shown in Fig. 6. The hardness of specimens in 5 μm deep (left edge point) became low because this affected by the influence of the surface edge.

The change of nitrogen concentration in Li before and after the test was negligibly small.

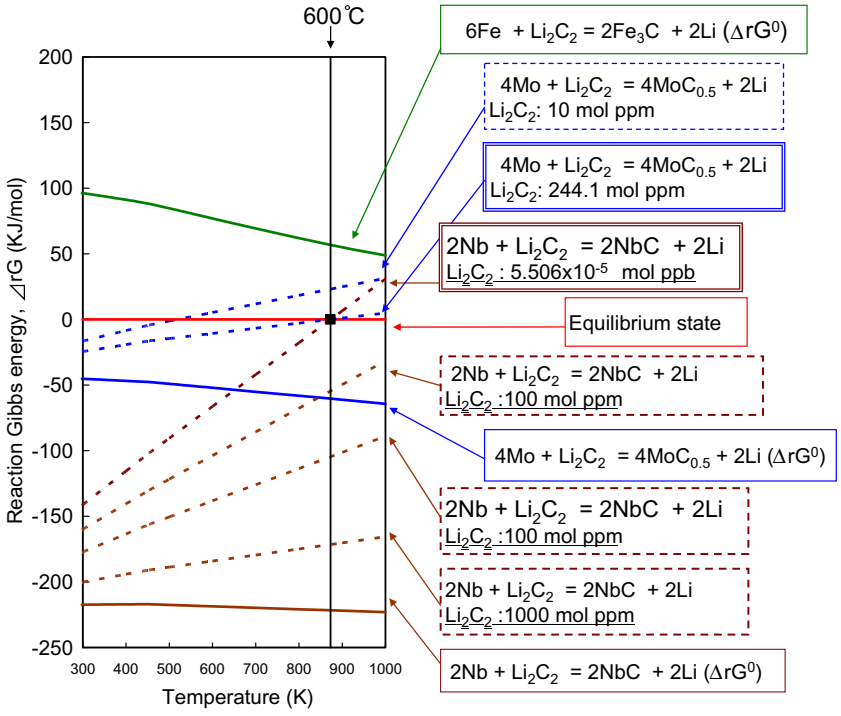


**Fig. 2.** Gibbs energy of chemical reaction on the crucible surface.

### 3.1. Corrosion of JLF-1 in Fe–9Cr crucible

The martensite lath structure which was seen before the exposure (Fig. 4E) disappeared on the surface of the specimens after exposure (Fig. 4A). The grain boundary in ferrite structure was observed on the surface without the etching procedure. This indicated that the grain boundary was locally corroded.

According to the EDS results, the depletion of Cr and W was detected on the surface of specimens corroded in the Li. The concentration of Cr on the surface decreased from 9% to 6–8% and the concentration of W decreased to half of that before the experiment. The development of ferrite layer could not be detected in depth direction. This indicated that the phase change was caused by Li only at the surface.

The weight loss was slightly smaller than those of previous studies [8,10]. The scattering of the data was smaller than that in the other tests, and this is possibly because the amount of precipitation and adherence of corrosion products were small.

Some possible corrosion products, such as $Li_2O$, $Li_9CrN_5$ are soluble in water and were removed during the cleaning.

### 3.2. Corrosion of JLF-1 in SUS316L crucible

Ni was accumulated on the specimen surface (white particle in Fig. 4B), which originated from SUS316L crucible and precipitated on the specimen surface. Ni of about 5 wt.% was detected on the surface. The precipitation possibly occurred in the cooling procedure due to the decrease of Ni solubility in Li. The

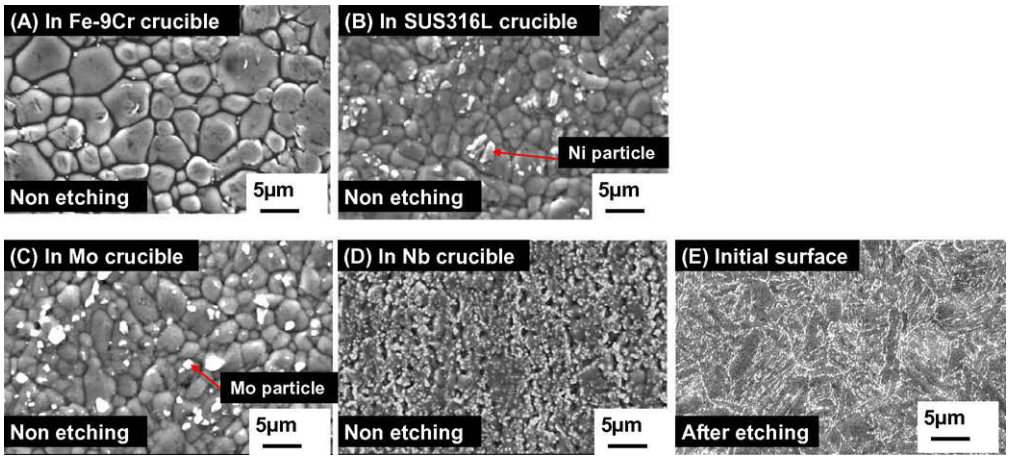


**Fig. 4.** SEM image of specimen surface tested in (A) Fe–9Cr, (B) SUS316L, (C) Mo, (D) Nb crucible and (E) before exposure.

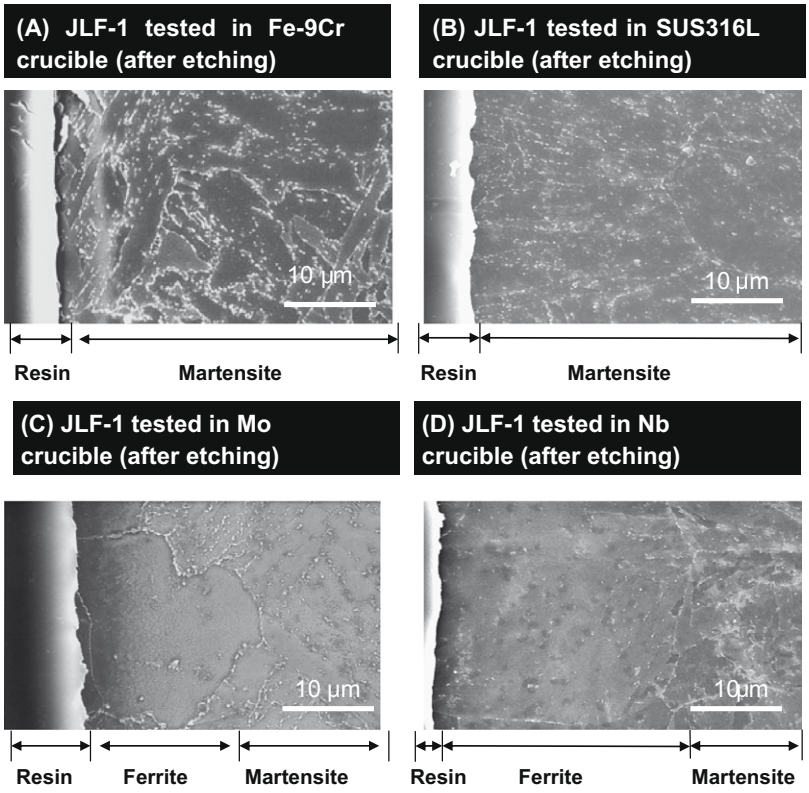


**Fig. 5.** Cross section of JLF-1 specimens after exposure in Li.

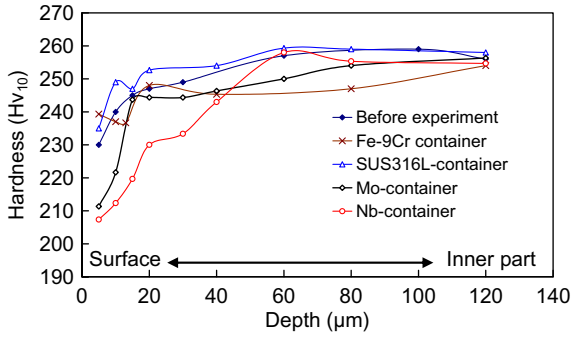


**Fig. 6.** Depth distribution of hardness after Li exposure in different crucibles.

results agreed well with that in previous results [8]. The data of the weight loss was not obtained because of the precipitation of large amount of Ni. The phase transformation was detected only on the surface similar to that obtained in Fe–9Cr crucible. This indicated that the Ni did not influence the phase transformation.

### 3.3. Corrosion of JLF-1 in Mo crucible

The specimen had nodules on the surface (Fig. 4C). The composition of these nodules was around 40% Mo, 50% Fe and 10% Cr by EDS analysis. These nodules were also observed in the previous corrosion tests performed using Mo containers [8]. The composition of the nodule is similar to those found in the present test. The size of the nodule at 700 °C in the previous study [8] was larger than that at 600 °C. This suggested that the growth of the nodules may be enhanced at high temperature.

The weight loss of the specimens was larger than that tested in Fe–9Cr steel, even though the corrosion products of Mo nodules were precipitated. The scattering of the data was larger than that in Fe–9Cr steel. This is because the amount of the precipitated Mo nodules was different in each specimen. The nodules were partly removed in the cleaning procedure.

The phase transformation was detected in the depth of 15 μm in average, which was quite difference from the results obtained in the crucible of Fe–9Cr steel and SUS316L. For the formation of the ferrite layer, carbon needed to be continuously depressed. Because the carbon concentration was low in Li, the concentration difference between liquid Li and specimen surface was the driving force for the dissolution. The carbon concentration and potential was controlled lower than that in the cases of Fe–9Cr steel and SUS316L crucible.

After the exposure, the reduction of hardness near the surface of specimen was detected (Fig. 6). The hardness drop from 250 to 210 Hv was detected on the surface. The depth where the hardness reduced was 20 μm, and this was consistent with the depth of the phase transformation.

### 3.4. Corrosion of JLF-1 in Nb crucible

The specimen had dimple surface due to the precipitation of Nb particles. The particles were small (Fig. 4D). The depth for the phase transformation was 30 μm in average, and twice larger than that in Mo case. This was possibly because lower carbon concentration in Li in Nb cup than that in Mo crucible had larger driving force for the carbon dissolution by larger concentration difference between the specimen and Li.

The depth of hardness reduction of the specimen surface was measured in Fig. 6 as 50 μm. This is deeper than that of the phase transformation. The area, where the phase transformation occurred, had a degraded property. The area beneath the area of the phase transformation also had a degraded property. This is possibly because the dissolution of carbon caused the degradation.

### 3.5. Corrosion model

Fig. 7 shows the model of the corrosion in the present study. The material element was dissolved from the specimens and the crucible. Here, the corrosion loss of JLF-1 is simply assumed to be dissolution of Cr and carbon. Then, the dissolution of Cr might be caused by the reaction [12] with Li and nitrogen;

$$5Li_3N(\text{in Li}) + Cr \rightarrow Li_9CrN_5 + 6Li. \quad (7)$$

The content of nitrogen in Li in the present study was 65 wppm and this corresponds to $1.29 \times 10^{20}$ atoms in Li. Here, it is assumed that nitrogen reacts with Cr on steel surface, and the corrosion product of $Li_9CrN_5$ is dissolved into Li. Then, Cr of $2.57 \times 10^{19}$ atoms could be dissolved in the Li, and this was dissolved Cr in total. This corresponds to the loss of $2.22 \times 10^{-3}$ g on the surface of the specimen and the crucible. Loss of weight in one specimen by the reaction of Eq. (7) is

$$L_s = \frac{S_s \times L_{total}}{S_c + n \times S_s}. \quad (8)$$

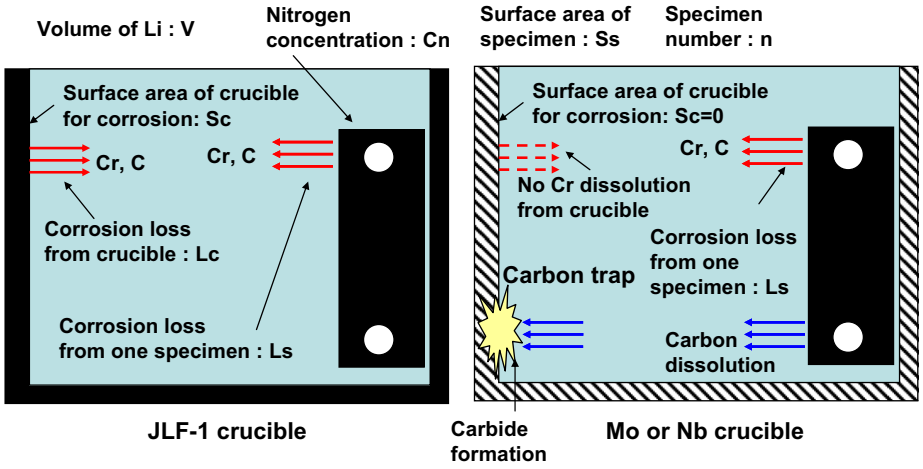


**Fig. 7.** Model of corrosion loss in static Li.

where $L_s$ and $L_{total}$ are the loss of Cr from one specimen and that in total including from the crucible, respectively. $S_c$ and $S_s$ is surface area of crucible and one specimen, respectively. $n$ is the number of specimens used in the test, and this is 10 in the present study.

In the test in Fe–9Cr crucible, the dissolution from the crucible was assumed to be the same as that from the specimen. Then, the weight loss of specimen per unit area was estimated as 0.186 g/m$^2$. The estimated weight loss was indicated by a dotted line in Fig. 3. In the test in Mo and Nb crucible, the weight loss was estimated by $S_c$ equal to zero based on the assumption that nitrogen does not reacts either Mo or Nb. Then, the weight loss of specimen per unit area was estimated as 0.806 g/m$^2$. The estimated weight loss was indicated as a solid line in Fig. 3. The difference of weight loss between these two lines was agreed with that obtained in the experiment. This indicated that the larger weight loss of specimen in Mo or Nb crucible was influenced by the corrosion of crucible.

The initial carbon concentration in JLF-1 is 0.1 wt.%. If the carbon concentration in zone of the phase transformation was nearly zero, the amount of the lost carbon from the specimen during the test in Mo and Nb crucible was roughly estimated to be $1.56 \times 10^{-4}$ g/m$^2$ and $3.12 \times 10^{-4}$ g/m$^2$, respectively. The influence of the loss of carbon on the weight loss was negligibly small. The effect of chemical potential of carbon on the dissolution of alloying elements of the steel was small.

## 4. Conclusion

Major conclusions are as follows:

1. Carbon potential in liquid lithium was controlled by the formation of stable carbide on the surface of crucible. In the test with Nb and Mo crucible, the carbon potential decreased by the trap of carbon on the crucible surface.
2. Weight losses of JLF-1 in Fe–9Cr crucible were small. The phase transformation from martensite to ferrite in the JLF-1 was observed just on the surface. The phase transformation was observed after the test in SUS316L crucible, where the concentration of dissolved Ni from the crucible into Li was high. The dissolved Ni did not affect on the phase transformation.
3. The depth of the phase transformation observed in JLF-1 after the test in Mo crucible was larger than that tested in crucible of Fe–9Cr and SUS316L. This was because the carbon potential in Li was reduced by the formation of Mo carbide.
4. The depth of the phase transformation observed after the test in Nb crucible was larger than that tested in Mo crucible. This was because the stability of the Nb carbide was larger than that of Mo carbide, resulting in lower carbon potential in Li, and larger driving force for the dissolution of carbon from the surface.

## Acknowledgment

This work was carried out based on NIFS Budget Code NIFS08UCFF004 and Grant-in-Aid for Scientific Research (A), (2007–2009) 19206100.

## References

[1] T. Muroga, M. Gasparotto, Fusion Eng. Des. 61–62 (2002) 13–25.
[2] A. Kohyama, T. Kohno, K. Asakura, H. Kayano, J. Nucl. Mater. 212–215 (1994) 684–689.
[3] P.F. Tortorelli, J. Nucl. Mater. 965–969 (1992) 191–194.
[4] P.F. Tortorelli, J.H. Devan, J. Nucl. Mater. 103–104 (1981) 633–638.
[5] Y.L. Wu, R.J. Pulham, M.G. Barker, J. Nucl. Mater. 172 (1990) 31–36.
[6] M.G. Barker, P. Hubberstey, A.T. Dadd, S.A. Frankham, J. Nucl. Mater. 114 (1983) 143–149.
[7] H. Sakaegawa, T. Hirose, A. Kohyama, Y. Katoh, T. Harada, K. Asakura, T. Kumagai, J. Nucl. Mater. 307–311 (2002) 490–494.
[8] Q. Xu, T. Nagasaka, T. Muroga, Fusion Sci. Technol. 52 (2007) 609–612.
[9] M. Nagura, M. Kondo, A. Suzuki, T. Muroga, T. Terai, Fusion Sci. Technol. 52 (2007) 630–634.
[10] Q. Xu, M. Kondo, T. Nagasaka, T. Muroga, M. Nagura, A. Suzuki, Fusion Eng. Des. 83 (2008) 1477–1483.
[11] O.K. Chopra, K. Natesan, T.F. Kassner, J. Nucl. Mater. 96 (1981) 269–284.
[12] R.J. Pulham, P. Hubberstey, J. Nucl. Mater. 115 (1983) 239–250.
[13] Thermodynamic Database MALT2, Kagaku Gijutsu-Sha, 2004.
[14] T. Sakurai, T. Yoneoka, S. Tanaka, A. Suzuki, T. Muroga, J. Nucl. Mater. 307–311 (2002) 1380–1385.